Electronic Supplementary Material (ESI) for Journal of Materials Chemistry A.

Supplementary Information

Highly elastic and mechanically robust polymer electrolytes with high ionic conductivity and adhesiveness for high-performance lithium metal batteries

1. Experimental section

Materials:

Bis(trifluoromethanesulphonyl)imide lithium salt (LiTFSI, 98%) was purchased from Adamas Reagent Co., Ltd. Poly(ethylene oxide) (PEO, M_w ca. 600 000 g mol^{-1}), N-methyl-2-pyrrolidione (NMP) and isophorone diisocyanate (IPDI) were purchased from Aladdin Reagent (Shanghai) Co., Ltd. Tetraethylene glycol dimethyl ether (TEGDME, 99%) was purchased from Sigma-Aldrich. N, N-Dimethylacetamide (DMAc, 99.8%, extra dry), ditin butyl dilaurate (DBTDL) and acetonitrile (99.9%, extra dry) were purchased from Sun Chemical Technology (Shanghai) Co., Ltd. 2-Amino-2-methyl-1, 3-propanediol (AMPD) was purchased from Acros Organics. Polyethylene glycol (PEG, M_n ca. 2000 g mol^{-1}) was purchased from Alfa Aesar. Polyvinylidene fluoride (PVDF), lithium iron phosphate ($LiFePO_4$) and acetylene black were purchased from Shenzhen Kejing Star Technology Co., Ltd. Lithium foils, copper foils and aluminum foils were purchased from Guangdong Canrd New Energy Technology Co., Ltd. All chemicals were used without further purification.

Preparation of the Li^+ ion-conductive polyurethane (PU) elastomer:

The typical synthetic procedure of the Li^+ ion-conductive PU elastomers is described below. First, PEG (2 g, M_n ca. 2 000 g mol^{-1}) was melted and stirred under vacuum at 110 °C for 2 h in a round bottom flask to remove the moisture residue and then cooled to 60 °C. LiTFSI salts were added into the liquid PEG and the PEG-LiTFSI mixture was then stirred at 60 °C for over 12 h, the molar ratio between the PEG ethoxy (EO) unit and LiTFSI was varied from 16:1, 12:1 to 8:1. After the complete dissolution of LiTFSI in the liquid PEG, IPDI (0.55 g), DBTDL (0.2 g) and anhydrous DMAc (5 mL) were mixed and then added into the PEG-LiTFSI mixture, followed by stirring for 3 h at 60 °C under a N_2 atmosphere. Thereafter, the DMAc solution of AMPD (0.87 g of AMPD dissolved in 10 mL of DMAc) was fed into the reaction system, followed by stirring for another 10 h at 50 °C. The resultant highly viscous product was cast into a glass mold and then dried at 80 °C overnight. The as-obtained transparent rubberlike sheet was then peeled off from the mold and further dried at 80 °C for 24 h under vacuum, resulting in the final Li^+ ion-conductive PU elastomer. For comparison, the pure PU sample without LiTFSI incorporated was prepared via a similar method.

Preparation of the PEO/LiTFSI complexes:

Specifically, 2 g of PEO (M_w ca. 600 000 g mol^{-1}) and 1.09 g of LiTFSI (the molar ratio between the PEO ethoxy (EO) unit and LiTFSI was 12:1) were dissolved in 20 mL of

acetonitrile under stirring at room temperature to obtain a homogeneous solution. The mixtures of PEO and LiTFSI were then cast into a Teflon mold, followed by volatilization of the acetonitrile. The as-obtained sample was further dried at 80 °C under vacuum for 24 h to remove the residual solvent, resulting in the PEO-LiTFSI complexes.

Preparation of the PU-EO/LiTFSI/TEG and PEO_{12}/LiTFSI/$TEG_{30\%}$ polymer electrolytes:

In an Ar-filled glovebox, the Li^+ ion-conductive PU elastomers and PEO/LiTFSI complexes were immersed in TEGDME for 20 min and 4 h, respectively, to obtain the final PU-EO/LiTFSI/TEG and PEO_{12}/LiTFSI/$TEG_{30\%}$ polymer electrolytes. The thickness of the polymer electrolytes ranges from 400 to 500 μm.

Characterization:

FTIR spectra were obtained with a Bruker VERTEX 80V FTIR spectrometer over the scanning range from 4000 to 400 cm^{-1} under vacuum. X-ray diffraction (XRD) measurements were conducted on a Rigaku SmartLab X-Ray diffractometer using Cu α radiation with the 2θ range of 3°-50° and collected with a step-width of 0.4° at room temperature. Differential scanning calorimetry (DSC) measurements were conducted on a TA instruments Q200 system at the heating/cooling rate of 20 °C min^{-1} in a N_2 atmosphere. Thermogravimetric analyses (TGA) were conducted using a TA Instruments Q500 thermogravimetric analyzer at the heating rate of 10 °C min^{-1} in a N_2 atmosphere. Tensile tests were performed on a universal testing machine (Instron 5944 Tension Instrument) at the stretching speed of 50 mm min^{-1} under ambient conditions (ca. 30% RH, 25 °C). Scanning electron microscopy (SEM) images were recorded on a Hitachi SU8020 SEM operated at 9 kV under vacuum.

Electrochemical measurements:

The coin-type Li||Li symmetric cells were assembled by sandwiching the PU-EO_{12}/LiTFSI/$TEG_{41\%}$ or PEO_{12}/LiTFSI/$TEG_{30\%}$ polymer electrolyte between two Li metal foils, followed by packaging in a CR2032 coin cell. The $LiFePO_4$ cathode was prepared by pasting a mixture of commercial $LiFePO_4$ powder, acetylene black and PVDF in NMP with a weight ratio of 8:1:1 on an Al foil. Then, the sample was dried at 80 °C for 12 h and subsequently punched into disks with diameters of 12 mm, wherein the areal loading of $LiFePO_4$ was ca. 1.4 mg cm^{-2} and 5.0 mg cm^{-2}. The Li metal foil was used as the anode. For the assembly of $LiFePO_4$||Li cells, the PU-EO_{12}/LiTFSI/$TEG_{41\%}$ or PEO_{12}/LiTFSI/$TEG_{30\%}$ electrolyte was sandwiched between the $LiFePO_4$ cathode and Li anode, followed by packaging into a CR2032 coin cell. The $LiFePO_4$||Li cell was charged and discharged between 2.5 and 4.0

V at varied current densities. The C rates in all the electrochemical measurements are defined based on 1C = 170 mA g^{-1}.

The $LiFePO_4$||Li pouch cell (7 × 8 cm^2) was assembled by sandwiching the PU-EO_{12}/LiTFSI/$TEG_{41\%}$ electrolyte between the $LiFePO_4$ cathode (mass loading of ca. 16.9 mg cm^{-2}) and thin Li anode (thickness of ca. 100 μm), followed by packaging by using the aluminum-plastic film. The Aluminum and the nickel tab is welded to the $LiFePO_4$ cathode and the thin Li anode using the tab ultrasonic welder, respectively. The $LiFePO_4$||Li pouch cell was charged at 0.01C in the voltage range from 2.5 to 4.0 V. All the batteries were assembled in an Ar-filled glove box. The cycling tests on the various cells were measured by the Land battery test system (CT2001, Wuhan Land Electronic Co. Ltd., China) at room temperature.

The ionic conductivity (σ) was measured by AC impedance spectroscopy using a PARSTAT MC 1000 multichannel electrochemical station (Princeton Applied Research, USA) in the frequency range from 1 MHz to 100 mHz at different temperatures. The ionic conductivity (σ) was calculated using the following equation:

$$\sigma = L/(R_b \times A_s) \qquad (1)$$

where R_b is the bulk resistance, L is the thickness of the polymer electrolyte, and A_s is the area of the symmetric electrode.

The experimental method for the measurement of ionic conductivity of the stretched polymer electrolytes is described as following. As shown in the figure below, the two ends of the polymer electrolyte were respectively fixed in two clamps, followed by stretching the sample to different strains of 100%, 200%, 300% and 400%. The two sides of the stretched polymer electrolyte were sandwiched by two stainless steel electrodes that can easily adhere to the sample due to its adhesive property. The stainless steel electrodes were connected to the electrochemical workstation and the electrochemical impedance spectra (EIS) were measured. Ionic conductivity (σ) of the polymer electrolyte at different strains was calculated based on the EIS using Equation (1):

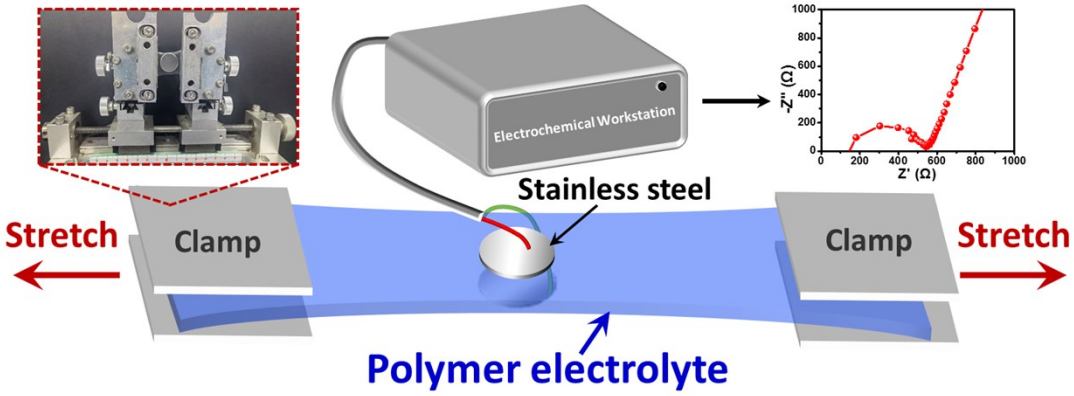

The lithium-ion transference number (t_{Li^+}) was measured by combining the chronoamperometry and EIS tests on the Li/Li symmetric cells with an applied voltage of 10 mV. The t_{Li^+} was calculated by the following equation:

$$t_{Li^+} = \frac{I_{SS}(\Delta V - I_o R_o)}{I_o(\Delta V - I_{SS} R_{SS})} \qquad (2)$$

where I_o and I_{SS} are the initial and steady-state current, ΔV is the step potential difference (10 mV), R_o and R_{SS} are the initial interfacial and steady-state interfacial resistance of the cell.

Linear sweep voltammetry (LSV) tests were carried out by sandwiching the PU-EO_{12}/LiTFSI/$TEG_{41\%}$ or PEO_{12}/LiTFSI/$TEG_{30\%}$ electrolyte between the stainless steel (SS, working electrode) and Li metal foil (reference and counter electrode) at room temperature. The voltage scan rate was 1 mV s^{-1} in the potential range from 3.0 to 6.0 V. Cyclic voltammetry (CV) measurements were carried out by sandwiching the PU-EO/LiTFSI/$TEG_{41\%}$ or PEO_{12}/LiTFSI/$TEG_{30\%}$ electrolyte between the $LiFePO_4$ electrode (working electrode) and Li metal foil (reference and counter electrode) at room temperature. The voltage was swept down from the open circuit potential to 2.5 V and then up to 4.0 V at a voltage scan rate of 0.1 mV s^{-1}.

The coin-type Li||Cu asymmetric cells were assembled by sandwiching the PU-EO_{12}/LiTFSI/$TEG_{41\%}$ or PEO_{12}/LiTFSI/$TEG_{30\%}$ polymer electrolyte between Cu and Li metal foils. The Cu foil was punched to the same diameter (1.6 cm) and surface area (2.01 cm^2) as the polymer electrolytes, while the surface area for the Li foil was 1.13 cm^2. Coulombic efficiency (CE) of the Li||Cu cells was tested via a repeated deposition and stripping method reported by Zhang's group (i.e., Method 3).[S1] Li was first deposited on Cu at a current density of 0.1 mA

cm^{-2} with a capacity of 1.0 mAh cm^{-2}, the cell was then charged and discharged for one cycle at a current density of 0.1 mA cm^{-2} with a total charge (Q_T) of 1.0 mAh cm^{-2}. After that, the cell was charged-discharged at 0.1 mA cm^{-2} with a cycled charge (Q_C) of 0.1 mAh cm^{-2} for n = 20 cycles, followed by final exhaustive stripping of the remaining Li reservoir to 1.0 V. The final stripping charge (Q_S), corresponding to the quantity of remaining Li after cycling, is measured. The average CE over n cycles (n = 20) can be calculated by the following equation:

$$CE_{avg} = \frac{nQ_C + Q_S}{nQ_C + Q_T} \quad (3)$$

Equation (4) can be applied if Equation (3) is attempted and all the Li reservoir is consumed during the Nth cycle (indicated by a rapid increase in overpotential) before the desired cycle number n is reached.

$$CE_{avg} = \frac{NQ_C}{NQ_C + Q_T} \quad (4)$$

Accordingly, Equation (3) with n = 20 is used for the Li||PU-EO_{12}/LiTFSI/$TEG_{41\%}$||Cu cell, while Equation (4) with N = 10 is used for the Li|| PEO_{12}/LiTFSI/$TEG_{30\%}$||Cu cell.

2. Supplementary figures and tables

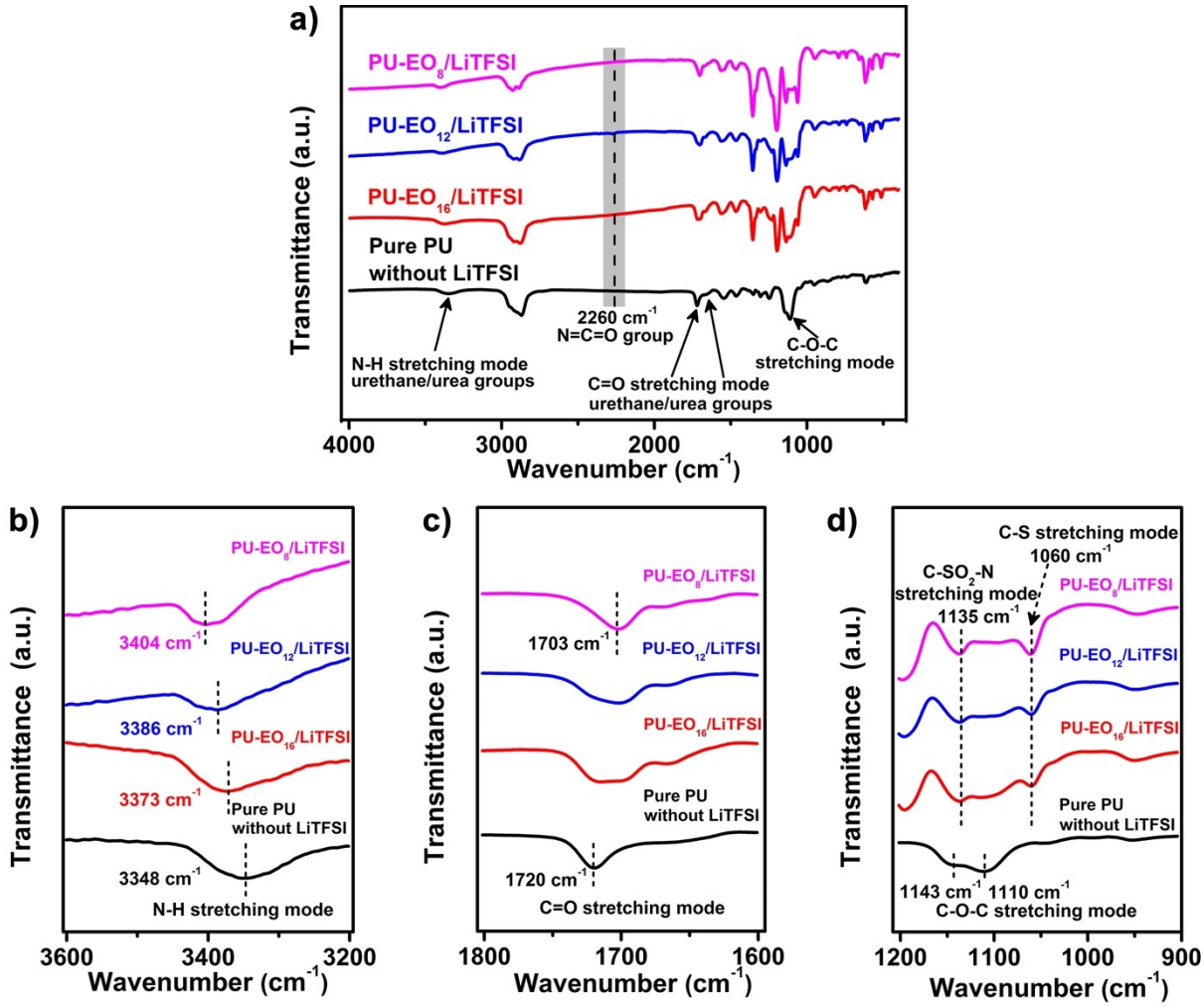

Fig. S1 FTIR spectra of the different PU-EO/LiTFSI elastomers and the pure PU sample without LiTFSI incorporated, in the wavenumber range of 4000-400 cm^{-1} (a), 3600-3200 cm^{-1} (b), 1800-1600 cm^{-1} (c) and 1200-900 cm^{-1} (d).

The FTIR spectra verify the chemical structures of the PU elastomers. The isocyanate (-NCO) stretching bands (2260 cm^{-1}) are completely disappeared for all the PU elastomers (Fig. S1a). This result suggests the formation of the three-dimensional poly(urethane-urea) network, resulting from the polycondensation reaction between the isocyanate groups of the prepolymer and the -OH/-NH_2 groups of AMPD (see Figure 1a in the main article). All the PU elastomers show characteristic FTIR peaks for the N-H stretching mode (Fig. S1b) and C=O stretching mode (Fig. S1c), suggesting the existence of urethane/urea groups in the PU elastomers. The

typical C-O-C stretching modes of the PEO segments are present at 1143 and 1110 cm^{-1} (Fig. S1d). In the FTIR spectra of the PU-EO/LiTFSI elastomers, the FTIR transmittance peaks of LiTFSI appear at around 1135 cm^{-1} and 1060 cm^{-1}, which are assigned to the C-SO_2-N stretching mode and C-S stretching mode, respectively.

The FTIR spectra also reveal the coordination interactions between the PU polymers and Li^+ ions. Compared to the pure PU sample without LiTFSI incorporated, the FTIR spectra of the PU-EO/LiTFSI elastomers exhibit following prominent changes: (i) the peak assigned to the N-H groups shifts to higher wavenumbers (Fig. S1b), (ii) the peak assigned to the C=O groups shifts to lower wavenumbers (Fig. S1c). (iii) The peaks assigned to the C-O-C groups are weakened, which is accompanied by the appearance of the peaks assigned to the C-SO_2-N and C-S groups from LiTFSI (Fig. S1d). All these results suggest that coordination interactions between the C=O/C-O-C groups and Li^+ ions occur in the PU-EO/LiTFSI elastomers.

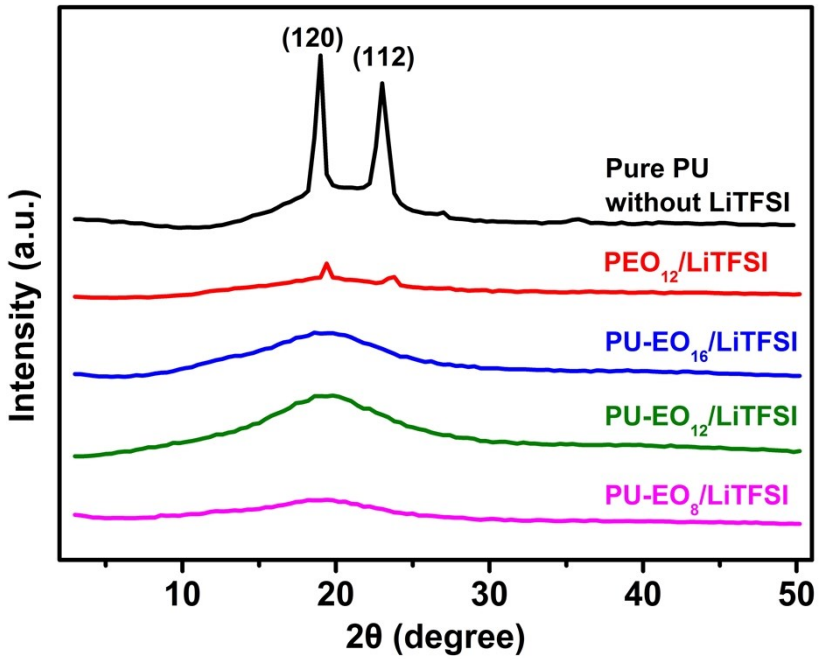

Fig. S2 XRD patterns of the pure PU sample without LiTFSI incorporated, the PEO_{12}/LiTFSI complexes and the different PU-EO/LiTFSI elastomers.

The XRD pattern of the pure PU sample shows two sharp diffraction peaks at 2θ of 19° and 23°, which are assigned to the (120) and (112) lattice planes of PEG crystals, respectively. The XRD pattern of the PEO_{12}/LiTFSI complexes also exhibits the diffraction peaks at 2θ of 19° and 23°, though their intensity is significantly decreased as compared to the pure PU sample. This result suggests that the PEG chains are also crystallized in the PEO_{12}/LiTFSI complexes. Comparatively, no sharp XRD peaks are detected for the PU-EO/LiTFSI elastomers, whereas broad humps, the representative XRD pattern of amorphous polymers, are detected for these samples. Therefore, the PEO chains are not crystallized in the PU-EO/LiTFSI elastomers.

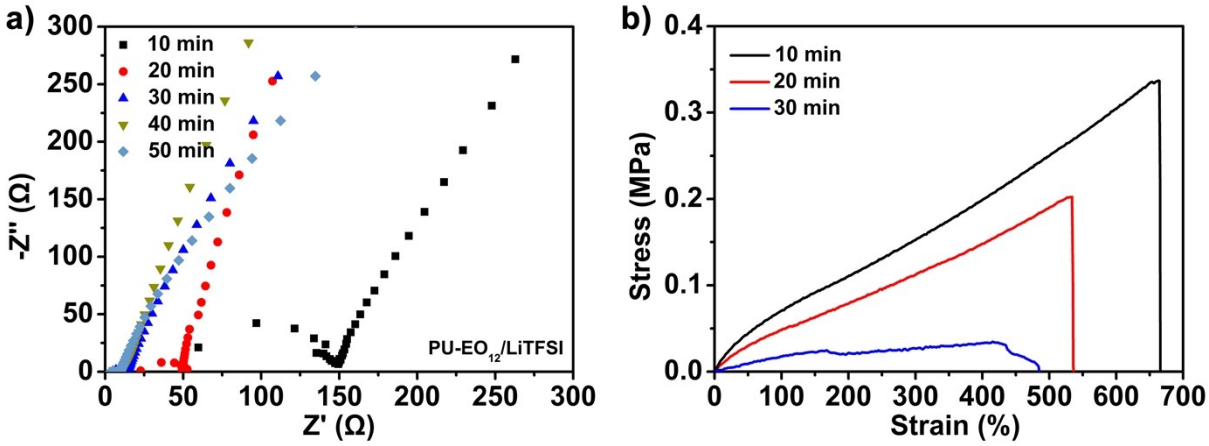

Fig. S3 (a, b) Nyquist plots determined from EIS (a) and stress-strain curves (b) of the PU-EO_{12}/LiTFSI polymer electrolytes, which were obtained by soaking the PU-EO_{12}/LiTFSI elastomers in TEGDME for different times. EIS were measured by the electrochemical workstation and used for the determination of the ionic conductivity.

Table S1. Summary of the plasticizer content, ionic conductivity and tensile strength of the PU-EO_{12}/LiTFSI polymer electrolytes as a function of the time used for soaking the PU-EO_{12}/LiTFSI elastomers in TEGDME.

Soaking time (min)	Plasticizer content (wt%)	Ionic conductivity (S cm^{-1})	Tensile strength (MPa)
10	30.6	1.7×10^{-4}	0.33
20	41.0	4.8×10^{-4}	0.20
30	50.7	5.4×10^{-4}	0.03
40	53.4	5.5×10^{-4}	*Too weak to measure*
50	53.0	5.5×10^{-4}	*Too weak to measure*

The ionic conductivity of the PU-EO_{12}/LiTFSI polymer electrolytes increases with the increase of soaking time from 10 min to 30 min and reaches the plateau after 30 min. However, the tensile strength of the PU-EO_{12}/LiTFSI polymer electrolytes decreases with the increase of soaking time. Among the different polymer electrolytes, the PU-EO_{12}/LiTFSI electrolyte resulting from the soaking time of 20 min shows well-balanced ionic conductivity (4.8×10^{-4} S cm^{-1}) and tensile strength (0.20 MPa).

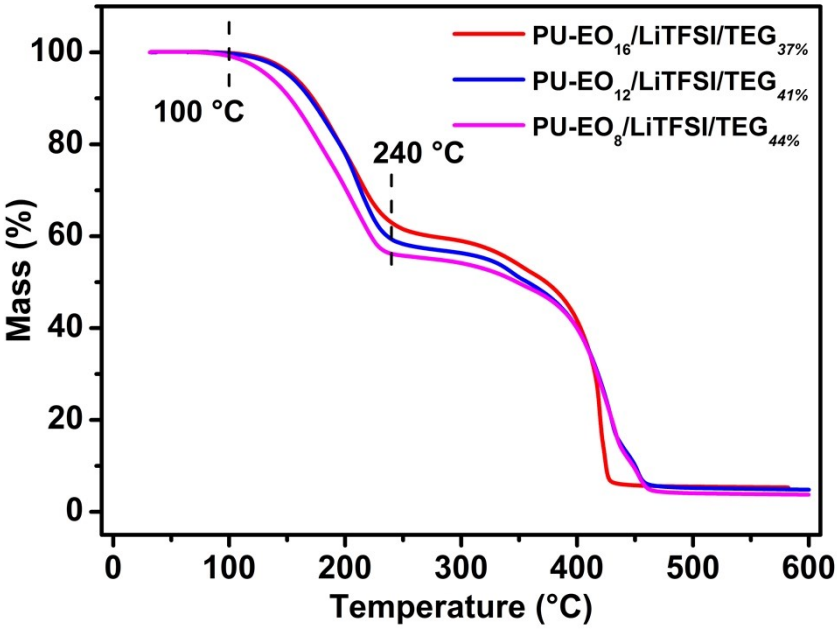

Fig. S4 TGA curves of the different PU-EO/LiTFSI/TEG polymer electrolytes.

The weight losses in the temperature range from 100 °C to 240 °C are ascribed to the volatilization of the TEGDME plasticizer. Accordingly, the weight contents of TEGDME in the PU-EO_{16}/LiTFSI, PU-EO_{12}/LiTFSI and PU-EO_8/LiTFSI-derived polymer electrolytes are measured to be 37%, 41% and 44%, respectively.

The contents of TEGDME in the polymer electrolytes were also measured by directly weighing the samples before and after soaking in TEGDME. In this way, the weight contents of TEGDME in the PU-EO_{16}/LiTFSI, PU-EO_{12}/LiTFSI, PU-EO_8/LiTFSI-derived polymer electrolytes are measured to be 37. 7 ± 1.9%, 40.4 ± 0.3%, 42.9 ± 1.3% respectively. The data are derived from the measurements of 3 baths of samples. It can be found that the as-measured values are quite similar to those measured by TGA.

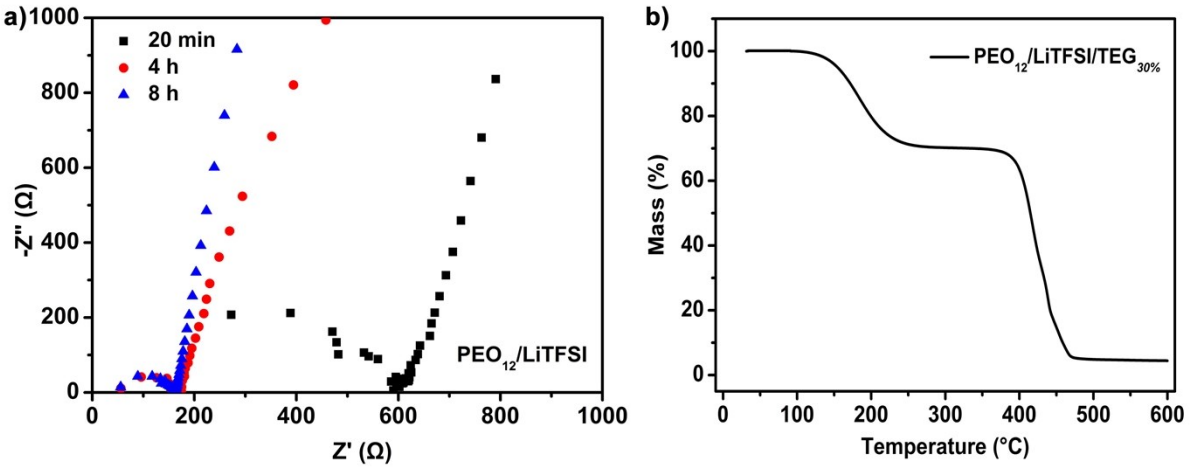

Fig. S5 (a) Nyquist plots of the PEO_{12}/LiTFSI polymer electrolytes, which were obtained by soaking the PEO_{12}/LiTFSI complexes in TEGDME for different times. (b) TGA curve of the PEO_{12}/LiTFSI/$TEG_{30\%}$ polymer electrolyte obtained by soaking the PEO_{12}/LiTFSI complexes in TEGDME for 4 h.

The ionic conductivity of the PEO_{12}/LiTFSI-derived polymer electrolytes increases with the increase of soaking time from 20 min to 4 h and reaches the plateau (1.8×10^{-4} S cm^{-1}) after 4 h. Therefore, the PEO_{12}/LiTFSI-derived polymer electrolyte, obtained by soaking the PEO_{12}/LiTFSI complexes in TEGDME for 4 h, is exclusively studied in this work. The weight content of TEGDME in the as-obtained polymer electrolyte is measured to be 30 wt% by TGA, which is quite similar to the result (30.3 ± 1.0%) measured by directly weighing the samples before and after soaking in TEGDME. Therefore, the as-obtained PEO_{12}/LiTFSI-derived polymer electrolyte is denoted as PEO_{12}/LiTFSI/$TEG_{30\%}$.

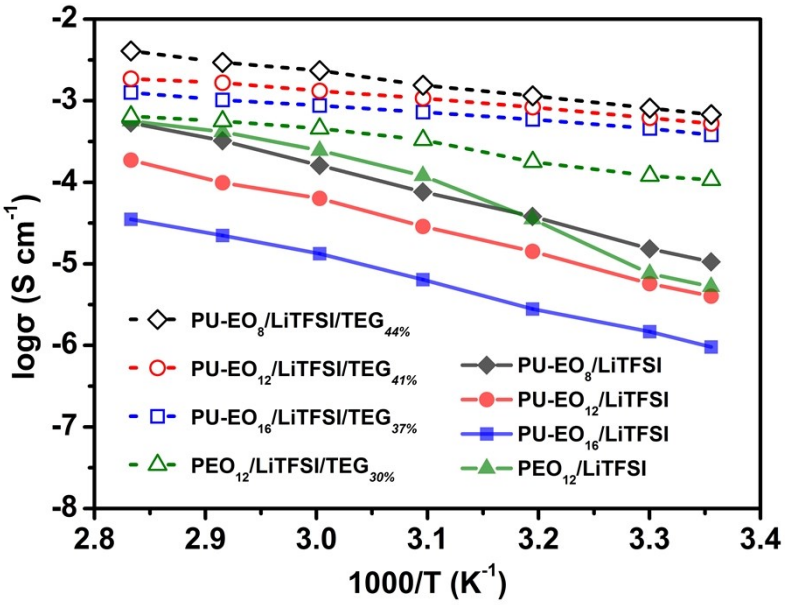

Fig. S6 Arrhenius plots of the TEGDME-free PU-EO/LiTFSI elastomers and PEO_{12}/LiTFSI complexes, and the different PU-EO/LiTFSI/TEG and PEO_{12}/LiTFSI/$TEG_{30\%}$ polymer electrolytes.

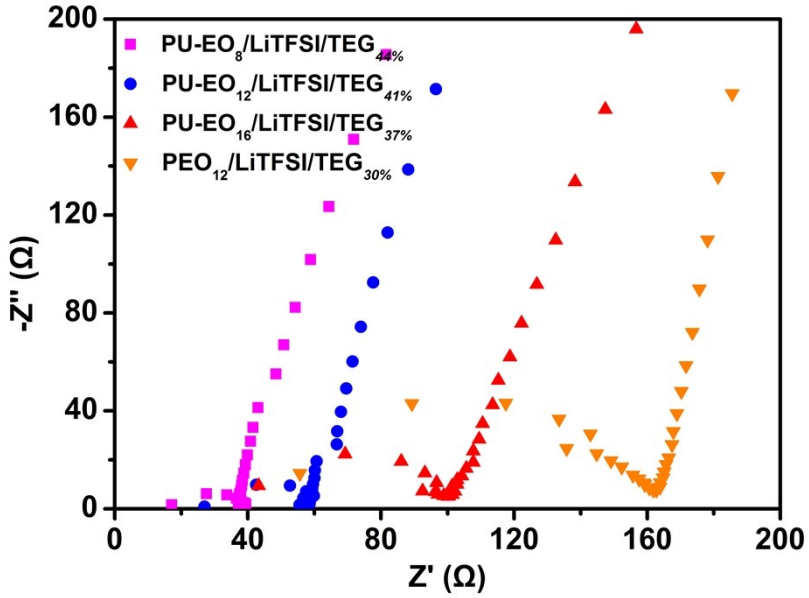

Fig. S7 Nyquist plots of the PU-EO/LiTFSI/TEG and PEO_{12}/LiTFSI/$TEG_{30\%}$ polymer electrolytes, which were measured by the electrochemical workstation and used for the determination of the ionic conductivity of the samples. The PU-EO/LiTFSI/TEG polymer electrolytes were obtained by soaking the corresponding elastomers in TEGDME for 20 min, while the PEO_{12}/LiTFSI/$TEG_{30\%}$ polymer electrolyte was obtained by soaking the PEO_{12}/LiTFSI complexes in TEGDME for 4 h.

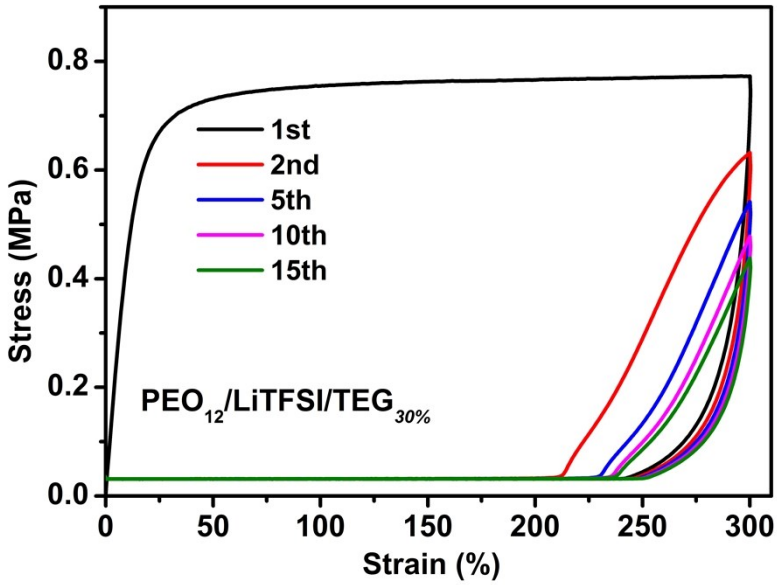

Fig. S8 Cyclic stress-strain curves of the PEO_{12}/LiTFSI/$TEG_{30\%}$ electrolyte, measured via the uninterrupted cyclic tensile tests at the strain of 300% for 15 uninterrupted loading-unloading cycles.

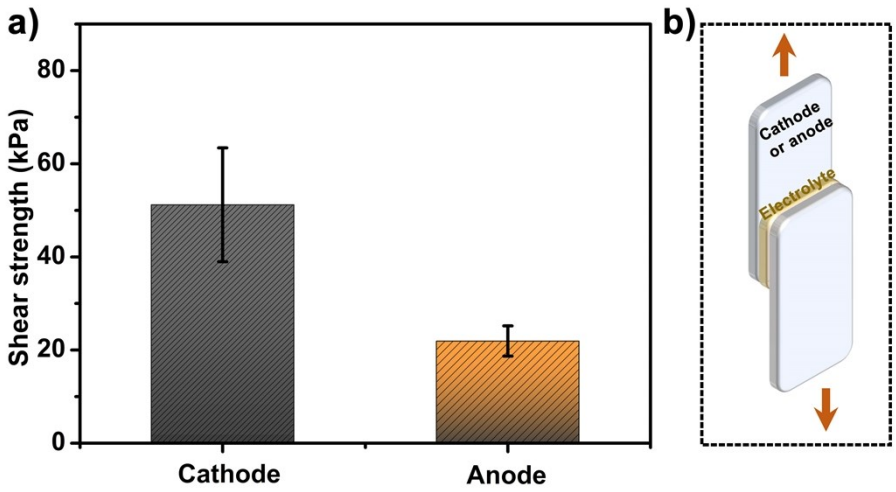

Fig. S9 (a) Shear strength of the lap joints of different electrodes bonded via the PU-EO_{12}/LiTFSI/$TEG_{41\%}$ electrolytes with thickness of ca. 400 μm. (b) Schematic illustration of the lap joints used for the measurement of shear strength.

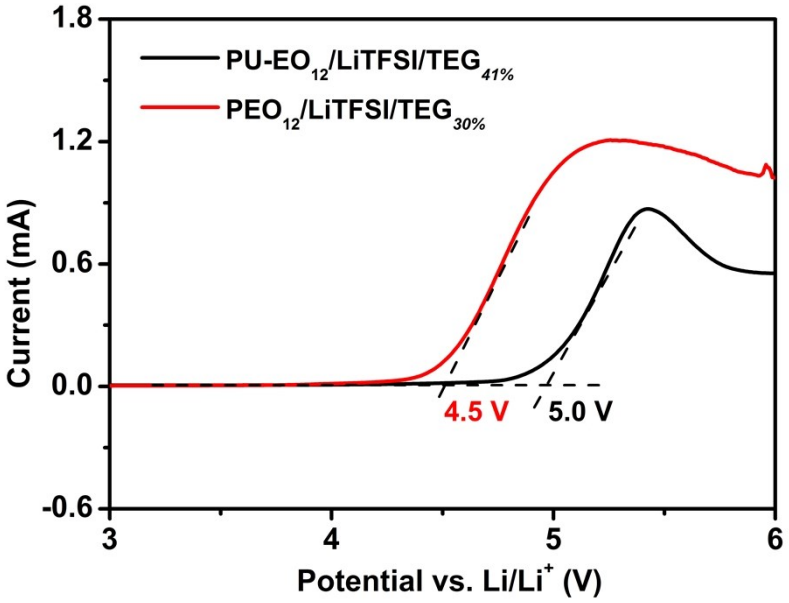

Fig. S10 LSV (from 3.0 to 6.0 V) profiles of the PU-EO_{12}/LiTFSI/$TEG_{41\%}$ and PEO_{12}/LiTFSI/$TEG_{30\%}$ polymer electrolytes at a scanning speed of 1 mV s^{-1}.

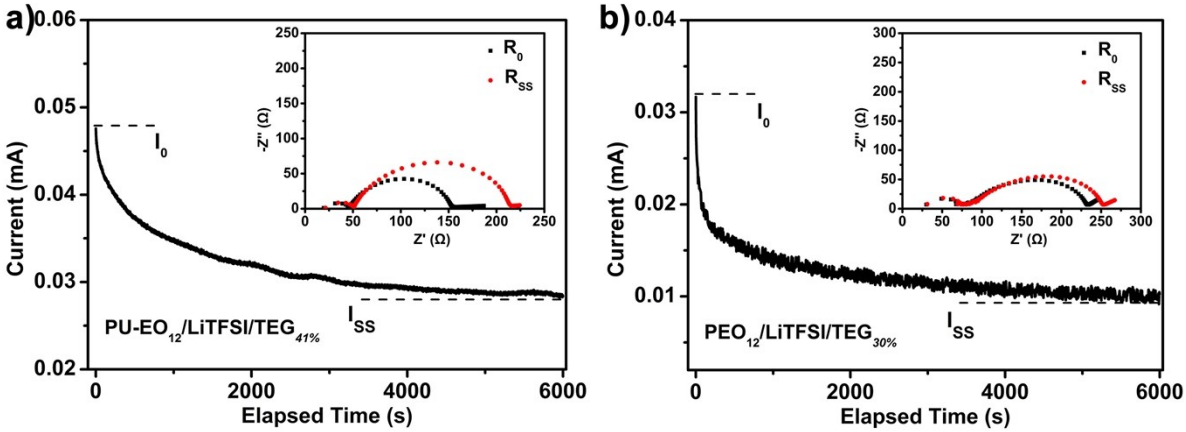

Fig. S11 (a, b) Chronoamperometry curves of the Li||PU-EO_{12}/LiTFSI/$TEG_{41\%}$||Li (a) and Li|| PEO_{12}/LiTFSI/$TEG_{30\%}$||Li cells (b), measured at a potential of 10 mV at room temperature. Insets: Nyquist plots of the cells before and after the chronoamperometry measurements.

Table S2. Summary of the lithium-ion transference numbers (t_{Li^+}) of the polymer electrolytes at room temperature and the parameters used for the calculation of t_{Li^+}.

Samples	I_0 (mA)	I_{SS} (mA)	R_0 (Ω)	R_{SS} (Ω)	t_{Li^+}
PU-EO_{12}/LiTFSI/$TEG_{41\%}$	0.0476	0.0284	155.8	216.1	0.40
PEO_{12}/LiTFSI/$TEG_{30\%}$	0.0317	0.00964	232.3	252.0	0.11

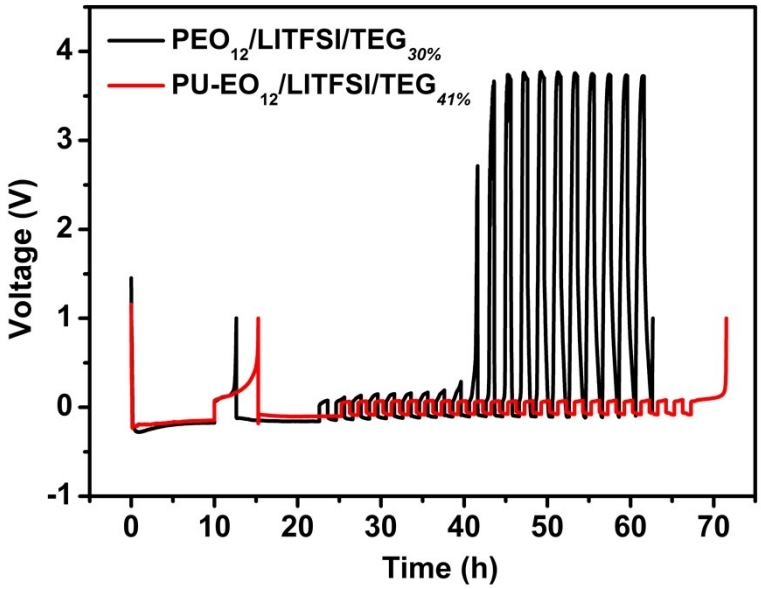

Fig. S12 Voltage versus time plots of Li||Cu asymmetric cells assembled with the PU-EO_{12}/LiTFSI/$TEG_{41\%}$ and PEO_{12}/LiTFSI/$TEG_{30\%}$ electrolytes.

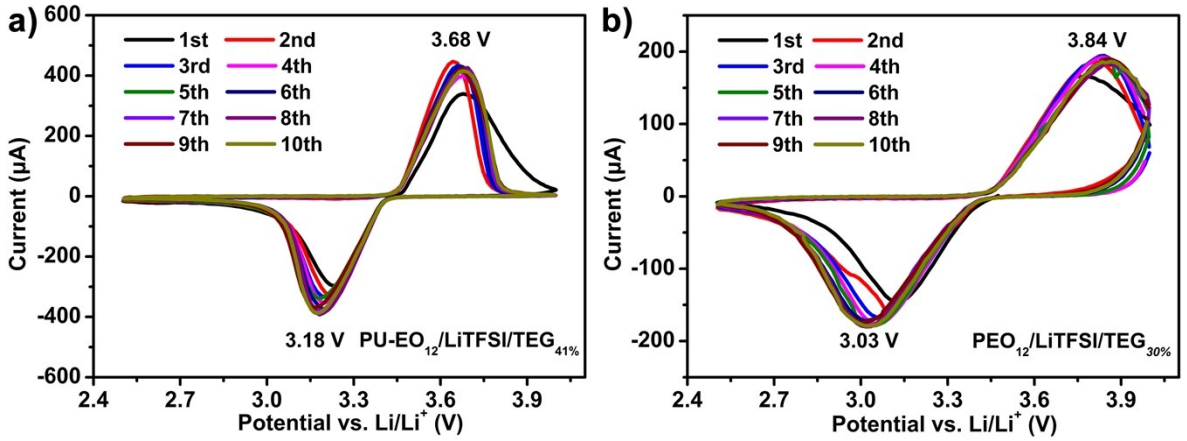

Fig. S13 (a, b) Cyclic voltammetry curves of the $LiFePO_4$||$PU\text{-}EO_{12}$/LiTFSI/$TEG_{41\%}$||Li (a) and $LiFePO_4$||PEO_{12}/LiTFSI/$TEG_{30\%}$||Li cells (b), measured at a scanning rate of 0.1 mV s^{-1} from 4.0 to 2.5 V.

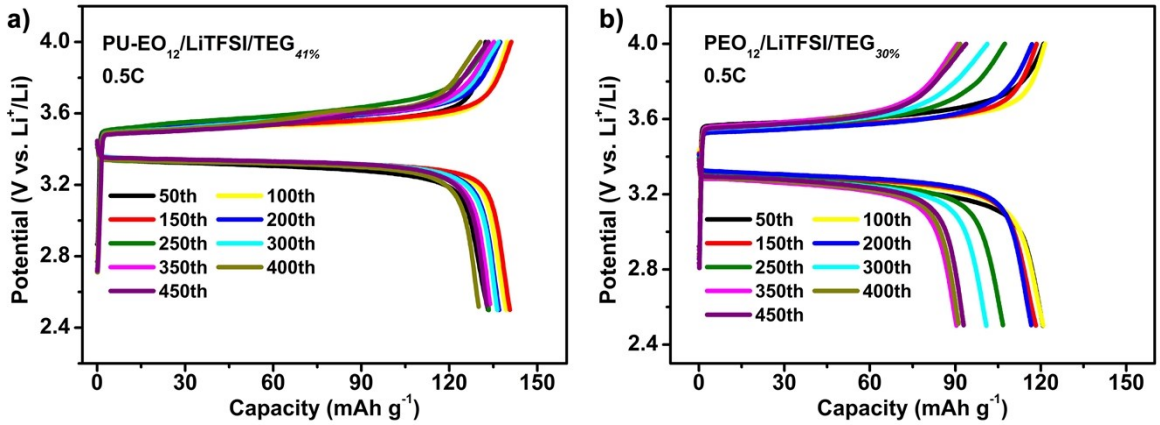

Fig. S14 (a, b) Typical galvanostatic charge/discharge voltage profiles versus cycle numbers of the $LiFePO_4$||PU-EO_{12}/LiTFSI/$TEG_{41\%}$||Li (a) and $LiFePO_4$||PEO_{12}/LiTFSI/$TEG_{30\%}$||Li (b) cells at 0.5C.

Table S3. Comparison of the rate capability and electrochemical cycling performances of the $LiFePO_4$||polymer electrolyte||Li cells and room-temperature ionic conductivity (*σ at RT*), between the PU-EO_{12}/LiTFSI/$TEG_{41\%}$ polymer electrolyte and the previously reported polymer electrolytes with elasticity. The rate capability and electrochemical cycling performances of the $LiFePO_4$||polymer electrolyte||Li cells were all measured at room temperature.

Polymer electrolytes	***σ at RT [S cm^{-1}]***	***$LiFePO_4$ Areal capacity [mAh cm^{-2}]***	***Rate capability***	***Discharge capacity and cycling performances***	***References***
PU-EO_{12}/LiTFSI/$TEG_{41\%}$	**4.8×10^{-4}**	**0.24**	**1C 127 mAh g^{-1}**	**0.2C 151 mAh g^{-1}**	**This work**
			4C 61 mAh g^{-1}	**0.5C 133 mAh g^{-1} 450 cycles**	
		0.85	**3C 85 mAh g^{-1}**	**0.2C 147 mAh g^{-1}**	
				0.5C 138 mAh g^{-1}	
SLIC-3 + 2 wt% SiO_2	1.2×10^{-4}	1.10	1C 71 mAh g^{-1}	0.2C 116 mAh g^{-1} 400 cycles	S2
ePPO	2.5×10^{-4}	0.60	2.5C 44 mAh g^{-1}	0.2C 152 mAh g^{-1} 300 cycles	S3
PTT	2.7×10^{-4}	0.25	1C 60 mAh g^{-1}	0.1C 140 mAh g^{-1}, 100 cycles	S4
PEO^B12K-POSS	9.8×10^{-5}	0.25	1C 83 mAh g^{-1}	0.2C 145 mAh g^{-1} 100 cycles	S5
SICPN	6.7×10^{-3}	1.50	1C 45 mAh g^{-1}	0.1C 108 mAh g^{-1} 50 cycles	S6

S1 B. D. Adams, J. Zheng, X. Ren, W. Xu and J-G. Zhang, *Adv. Energy Mater.*, 2018, **8**, 1702097

3. Supplementary references

S2 D. G. Mackanic, X. Yan, Q. Zhang, N. Matsuhisa, Z. Yu, Y. Jiang, T. Manika, J. Lopez, H. Yan, K. Liu, X. Chen, Y. Cui and Z. Bao, *Nat Commun*, 2019, **10**, 5384.

S3 J. Lopez, Y. Sun, D. G. Mackanic, M. Lee, A. M. Foudeh, M. S. Song, Y. Cui and Z. Bao, *Adv Mater*, 2018, **30**, 1804142.

S4 Y. Zhang, W. Lu, L. Cong, J. Liu, L. Sun, A. Mauger, C. M. Julien, H. Xie and J. Liu, *J. Power Sources*, 2019, **420**, 63-72.

S5 W. Wei, Z. Xu, L. Xu, X. Zhang, H. Xiong and J. Yang, *ACS Appl. Energy Mater.*, 2018, **1**, 6769-6773.

S6 T. Dam, S. S. Jena and A. Ghosh, *J. Appl. Phys.*, 2019, **126,** 105104.